A two stage Polynomial Chaos Expansion application for bound estimation of uncertain FRFs

Murat Kara[1,2*] and Neil S Ferguson[2*]

[1]Department of Mechanical Engineering, Bolu Abant Izzet Baysal University, Turkey

[2]Institute of Sound and Vibration Research, University of Southampton, UK

[*]e-mail: kara.murat@ibu.edu.tr, nsf@isvr.soton.ac.uk

ABSTRACT

Polynomial Chaos Expansion (PCE) is a method for analysing uncertain vibratory structures with lower computational effort. It may simply be described as a curve fitting method with orthogonal basis terms, where the polynomial type, dimension and order are predefined for the uncertain responses. However, the polynomial order in PCE must be very high to accurately estimate statistical moments of the frequency response function in resonance regions of lightly damped and uncertain structures. To solve this issue different transformation techniques are reported in the literature, where implementations of PCE produce higher accuracy with a lower order polynomial. However, these transformations lose the attraction for using PCE, since they require some additional mathematical operations and, mostly, they present high accuracy if the higher orders of polynomials are again of interest. In this study, an efficient approach is presented for the upper bound estimation of the uncertain frequency response functions (FRFs) via PCE with lower order terms without performing any transformation. Rather than one-stage application of PCE for the desired response of an uncertain problem, the approach comprises a two-stage application of the classical PCE, i.e. first for the natural frequencies and then for the FRF calculations. As an example application of the approach, a thin beam for two different uncertainty cases is considered, namely local and global uncertainty. The local and global input uncertainties are generated by variability of lumped masses added at the boundary and Young's

modulus, respectively. The FRF bounds are compared with extensive experimental and numerical Monte Carlo simulations, showing that low order polynomials are sufficient to calculate the bounds accurately with the technique described.

Keywords: Polynomial Chaos Expansion, bound estimation, frequency response function, uncertainty

1 INTRODUCTION

Uncertainties naturally arise in every field of engineering practice. However, disregarding these uncertainties in the analyses may cause undesirable results with both time and cost losses. To avoid these losses, uncertainty must be taken into account from the design stage. For this reason, researchers continue to study uncertainty analysis.

Since uncertainty is very effective on the subsequent dynamic responses, studies are carried out in this area as well. For this purpose, many different methods such as Monte Carlo simulation [1], interval analysis [2,3], anti-optimization [4] and reliability analyses [5,6] have been introduced and all these methods have their own advantages and disadvantages. Among these methods, Polynomial Chaos Expansion (PCE) is one of the most frequently used methods [7]. PCE can basically be defined as fitting a polynomial curve to the uncertain response. The method has several advantages. The first of these is the modelling capability of different distribution types such as normal, uniform, beta or gamma distributions. In this context, any distribution of an uncertain parameter can be modelled with a desired polynomial type. However, if the appropriate type of polynomial corresponding to the distribution type of the uncertain parameter is selected, the uncertain parameter is expressed as a very low-order polynomial and the computational time shortens and also the accuracy of the method increases. In addition, the deterministic coefficients of the polynomial can be obtained with different methods such as Galerkin projection, collocation, and a statistical moment approach. In simple

applications of PCE, the Galerkin projection approach can be used however it can be tedious for uncertainty analysis of complex models. Therefore, the collocation point method is widely used as a non-intrusive method in more complex models. There are studies on the selection of the collocation points via Latin Hypercube sampling [8,9]. It is also convenient to use the roots of the higher order polynomial basis to be adopted, as reported by Henneberg et al. [10].

Another advantage of PCE is the capability of using it together with either analytical or numerical solution methods. Thus, its applicability to simple and complex models is increasing. In this context, the success of the method with analytical calculations is demonstrated by Henneberg et al. [10] and Jacquelin et al. [11,12]. Besides, Ghanem and Spanos described using PCE with the finite element (FE) method, abbreviated as FE-PCE, in detail [7]. Since FE is widely used in industry, the application of FE-PCE has become quite common [13–15]. On the other hand, Manan and Cooper [8] obtained FE matrices of a bending beam and an airplane wing and used them in the calculation of the bounds of the forced vibration response via PCE. PCE has also been utilized in the analysis of uncertain structures together with different numerical solvers. In this regard, Sarkar and Ghanem [16,17] examined the mid-frequency FRF response of an uncertain structure by combining PCE together with numerical methods. The structure is divided into substructures by a proper orthogonal decomposition, where the uncertainty of the individual structures on the complex structure is taken into account at this stage [16]. Sarsri et al. [18] used component mode synthesis to reduce the size of large FE models and then solved the uncertain problem via PCE. Concerning wave approaches, Sepahvand et al. [19] solved the one-dimensional uncertain wave equation by combining PCE with the finite difference method. Also, Henneberg et al. [10] implemented PCE together with the wave finite element method for the width and the centre frequency for the bandgaps of periodic structures. More recently, Secgin et al. [20] showed that PCE can be reliably combined

with the discrete singular convolution for the probability density function (PDF) of the natural frequency of uncertain non-uniform beams.

PCE is also used to mathematically express the uncertainty obtained from experimental data. In this regard, Sepahvand and Marburg [21] calculated the uncertain material properties of composite plates from experimental modal data and modelled them by PCE. In a later study, Sepahvand [22] determined the uncertain damping ratios of the composite plates by experimental modal analysis. Then, by calculating the PDF from the samples obtained, the uncertain frequency response functions (FRFs) were calculated by FE-PCE [22].

The studies referred to in the above clearly demonstrates that PCE is successful for the estimation of natural frequencies [13,20,23] and vibration amplitude at non-resonant frequencies [12] of the structures and the frequency bandwidth and bandgap centre frequencies [10].

In some uncertainty quantification problems via PCE, the polynomial order must be very high to produce an accurate estimation. For this purpose, there are different procedures utilized in PCE to reduce the order of the polynomial. In this regard, Blatman and Sudret [24] exploited least angle regression to detect the most effective deterministic coefficients for PCE on the desired response, which enable one to obtain an adaptive sparse polynomial. Keshavarzzadeh et al. [25] examined two sequence transformations, namely Shank's and Levin transformations, to accelerate the convergence of PCE. The requirement for a higher order polynomial expansion is also encountered in estimating the FRF around the resonance of uncertain vibratory structures having low damping. The classical implementation of PCE with low order polynomials is not able to estimate the mean and variance of the response FRF at resonance frequencies for such structures, as reported by Jacquelin et al. [12,26]. Therefore, different approaches must be implemented to solve this issue. In this regard, Jacquelin et al. [11] implemented three different transformations, i.e., Aitken's transformation, recursive Aitken's transformation and Shank's

transformation, for the statistical moments of the response. Similarly, Yaghoubi et al. [27] used stochastic frequency transformation. Although these transformations produce reliable results in uncertainty estimations of vibratory structures, PCE loses its attraction due to the need to use some additional mathematical operations and expansion resulting in increased computational time.

Here, an efficient approach is presented for the upper bound estimation of the uncertain FRFs via the classical PCE with lower order terms without performing any transformation. The method is tested for the beams having different uncertainty cases, i.e., local and global uncertainty. Local uncertainty is generated by adding variable lumped mass at the free boundary of a cantilever beam, whereas the global case is performed by considering the beam possessing an uncertain Young's modulus. The first uncertainty case is also experimentally verified. Even though two cases are examined, the application of the approach is the same. The approach consists of a two-stage PCE application to determine the bounds, rather than the direct application of PCE for the FRF as reported in the literature. At the first stage, PCE is utilized to compute the PDF of the natural frequencies in the considered frequency range. The subsequent stage is the estimation of the uncertain FRFs. Although a finite element model of the beam is utilized as a numerical solver in the computations, one may construct the model by any numerical method, but note that, it must be able to compute the natural frequency and FRF for the considered structure. The results of the presented approach are compared with Monte Carlo simulation. Besides, PCE is tested without using the introduced approach by calculating the mean FRF and FRF bound together without implementing Shank's transformation, whereas the mean FRF is also checked using Shank's transformation. It is seen that the proposed approach has a good accuracy on the upper bound estimation, even in the cases where the mean FRF estimations fail via the application of PCE with Shank's transformation, namely for the global uncertain beam.

2 POLYNOMIAL CHAOS EXPANSION

2.1 Modelling of an uncertain variable

According to Polynomial Chaos Expansion (PCE), any uncertain input/output variable (X) can be represented as follows [7]:

$$X = \sum_{j=0}^{\infty} x_j P_j(\xi) \approx \sum_{j=0}^{N} x_j P_j(\xi), \tag{1}$$

where ξ is an uncertain parameter, x_j is deterministic coefficient of the polynomial and $P_j(.)$ is orthogonal polynomial by which the uncertain variable is to be represented. As shown in Eq. (1), PCE of an uncertain variable is theoretically extended up to infinity. However, it is truncated at a finite number (N) in numerical computations [13]:

$$N = \frac{(n+p)!}{n!\,p!} - 1. \tag{2}$$

Here, n and p denote the number of uncertain parameter and the order of the polynomial. In PCE, polynomial terms used to represent the uncertain variable are orthogonal to each other [7]:

$$\left\langle P_i \cdot P_j \right\rangle = \delta_{ij} \left\langle P_j^2 \right\rangle. \tag{3}$$

Here, $\langle\ \rangle$ represents the mean value and δ_{ij} denotes Kronecker delta function. Due to the orthogonality of the polynomials, it is easy to calculate the statistical moments of the uncertain variable. The mean and variance of the results may be calculated by,

$$\mu_X = x_0, \tag{4}$$

and

$$\sigma_X^2 = \sum_{j=1}^{N} x_j^2 \left\langle P_j^2 \right\rangle, \tag{5}$$

respectively.

In PCE, many types of orthogonal polynomials may be utilized, i.e., Hermite, Laguerre, Jacobi, Legendre, etc. As reported by Xiu and Karniadakis [28], each polynomial type efficiently models a certain type of probability distribution as the weighting functions of the polynomial basis coincide with mathematical expressions of the probability distribution types. Using the efficient polynomial basis-distribution type couple is called as optimal representation. For the optimal representation, one may utilize Hermite, Laguerre, Jacobi and Legendre polynomial bases for normal, gamma, beta and uniform distributions, respectively. For the optimal representation, a linear polynomial is enough to represent the uncertain variable. If an appropriate polynomial basis-distribution type is not used, it is called a "non-optimal representation" and higher order terms of polynomials are required [13]. In non-optimal cases, a space transformation is required to derive the uncertain variable, more terms are necessary in the expansion.

In Eq. (1), different types of polynomials can be used for the function set P, i.e., nth order Hermite and Legendre polynomial terms are respectively calculated by [13]:

$$P_n\left(\boldsymbol{\xi}\right)=\left(-1\right)^n e^{\frac{1}{2}\boldsymbol{\xi}^T\boldsymbol{\xi}}\frac{\partial^n}{\partial\xi_{i_1}\partial\xi_{i_2}...\partial\xi_{i_n}}e^{-\frac{1}{2}\boldsymbol{\xi}^T\boldsymbol{\xi}}, \tag{6}$$

$$P_n\left(\boldsymbol{\xi}\right)=\frac{\left(-1\right)^n}{n!2^n}\frac{\partial^n}{\partial\xi_{i_1}\partial\xi_{i_2}...\partial\xi_{i_n}}\left(1-\boldsymbol{\xi}^T\boldsymbol{\xi}\right)^n. \tag{7}$$

In PCE, there are types of approaches such as Galerkin projection, the collocation method to determine the unknown deterministic coefficients shown in Eq. (1). In the present study, the collocation method is utilized.

2.1.1 *Space transformation for an uncertain input variable*

If the uncertain parameter ξ is defined in the interval of $\xi \in [a,b]$ and uncertain input physical variable X is defined between $X \in [c,e]$, then a space transformation is required to derive the uncertain variable X in terms of uncertain parameter ξ [13]:

$$\int_c^X d_1(\tau)\,d\tau = \int_a^\xi d_2(\tau)\,d\tau \Rightarrow X = f(\xi). \tag{8}$$

Here, d_1 and d_2 represent the PDF of the uncertain parameter and physical variable, respectively. For optimal representation, this procedure reduces to a simple shifting. A normally distributed uncertain variable (X) with the statistical properties, $N(\mu_X, \sigma_X)$, may be represented by a first order polynomial of an uncertain parameter, ξ, if the optimal polynomial basis i.e., Hermite polynomial basis is selected for the representation:

$$X = \sigma_X \xi + \mu_X, \tag{9}$$

where μ_X and σ_X are the mean and standard deviation of the uncertain variable and uncertain parameter has a standard normal distribution, $N(\mu_\xi, \sigma_\xi) = N(0,1)$. For non-optimal representation, it may be difficult to obtain a simple expression as Eq. (9) and therefore, one may also utilize different methods which will be mentioned in following subsection to calculate the deterministic coefficients of an input variable.

2.2 Calculation of the deterministic coefficients in PCE

In the literature, there are different methodologies to calculate the deterministic coefficients [10,13,24]. In this study, the collocation method is utilized since it is a non-intrusive method and convenient for complex problems.

In the collocation method, a set of uncertain parameters ($\boldsymbol{\xi} = \left\{ \xi^{(1)} \quad \xi^{(2)} \quad \cdots \quad \xi^{(N_{CP})} \right\}^T$) is sampled and corresponding uncertain variable realizations ($\mathbf{X} = \left\{ X^{(1)} \quad X^{(2)} \quad \cdots \quad X^{(N_{CP})} \right\}^T$) is calculated. It should be mentioned that the number of collocation points (N_{CP}) should be equal or greater than number of the finite terms (N+1). Substituting the samples of the collocation points and realizations into Eq. (1) yields a set of linear equations with unknown deterministic coefficients [9,10]:

$$\mathbf{P}\mathbf{x} = \mathbf{X} \ , \tag{10}$$

where,

$$\mathbf{P} = \begin{bmatrix} P_0\left(\xi^{(1)}\right) & P_1\left(\xi^{(1)}\right) & \cdots & P_N\left(\xi^{(1)}\right) \\ P_0\left(\xi^{(2)}\right) & P_1\left(\xi^{(2)}\right) & \cdots & P_N\left(\xi^{(2)}\right) \\ \vdots & \vdots & \ddots & \vdots \\ P_0\left(\xi^{(N_{CP})}\right) & P_1\left(\xi^{(N_{CP})}\right) & \cdots & P_N\left(\xi^{(N_{CP})}\right) \end{bmatrix}_{N_{CP}\times(N+1)} \ , \tag{11}$$

and $\mathbf{x} = \left\{ x_0 \quad x_1 \quad \ldots \quad x_N \right\}^T$ is the vector of deterministic coefficients. It is seen, Eq. (11) is a square matrix if number of collocation points equals to number of the terms in PCE. If a higher number of collocation points are utilized, the deterministic coefficients are calculated by [9],

$$\mathbf{x} = \left(\mathbf{P}^T\mathbf{P}\right)^{-1}\mathbf{P}^T\mathbf{X} \ . \tag{12}$$

The selection of the collocation points is another issue for this method. One of the most efficient ways is selecting the roots of $(N+1)^{th}$ order of basis polynomial, i.e., roots of the 3rd order Legendre polynomial may be selected as the collocation points for the determination of the 2nd order of the same polynomial coefficients.

2.3 Transformations for increasing the convergence of PCE

The reason for the need of transformations in PCE was described in the introduction. In this study, Shank's transformation is utilized. For the brevity of the study, suppose that M_p is any

statistical moment (mean, variance and third order statistical moment) of the FRF at a certain frequency obtained using PCE with order p. The rth order Shank's transformation (e_r) is expressed as follows [11]:

$$e_r = \frac{\begin{vmatrix} M_p & M_{p+1} & \cdots & M_{p+r} \\ M_{p+1} & M_{p+2} & \cdots & M_{p+r+1} \\ \vdots & \vdots & \cdots & \vdots \\ M_{p+r} & M_{p+r+1} & \cdots & M_{p+2r} \end{vmatrix}}{\begin{vmatrix} \Delta^2 M_p & \Delta^2 M_{p+1} & \cdots & \Delta^2 M_{p+r-1} \\ \Delta^2 M_{p+1} & \Delta^2 M_{p+2} & \cdots & \Delta^2 M_{p+r} \\ \vdots & \vdots & \cdots & \vdots \\ \Delta^2 M_{p+r-1} & \Delta^2 M_{p+r} & \cdots & \Delta^2 M_{p+2r-2} \end{vmatrix}}. \tag{13}$$

Here $\Delta^2 M_p = M_{p+2} - 2M_{p+1} + M_p$. The workflow of Shank's transformation is presented in Fig. 1. It may be observed from Eq. (13) or the flow diagram presented in Fig. 1 that, this transformation requires the evaluation of M_i where $i=\{p, p+1, \ldots, p+2r\}$. This procedure increases the computational load and hence loses the attraction for using PCE, since the procedure to calculate the coefficients is repeated for $2r+1$ times with an increasing order of terms.

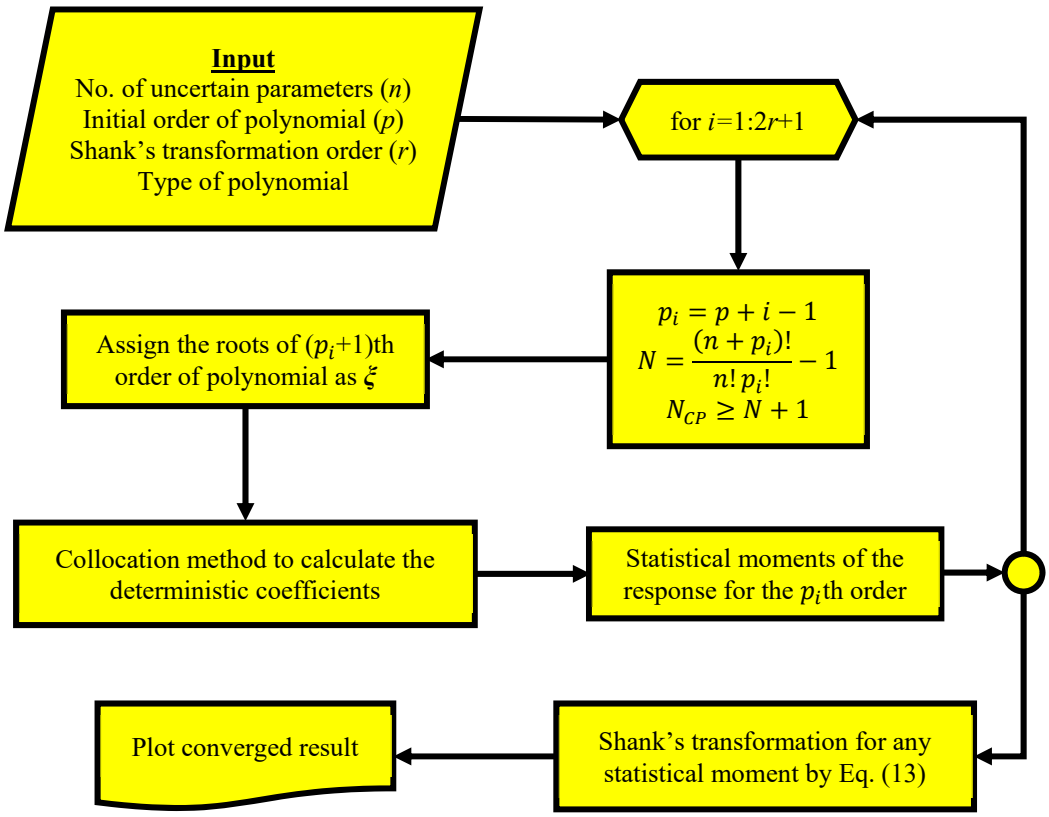

Figure 1. Workflow of Shank's transformation in PCE

2.4 Modal based PCE approach for the upper bound of frequency response function

In the literature, PCE is directly implemented for the desired statistical moment of the response, referred to here as a one-stage application of PCE in this paper. With the one-stage application of PCE, the statistical moments of the lightly damped and uncertain structures produce fluctuations at frequencies around the natural frequency, as reported by Jacquelin et al. [12]. In this section, an implementation of PCE for the upper bound estimation of frequency response function (FRF) over a certain frequency range, [f_l, f_u], is described. The approach mainly determines the bounds by breaking down the whole frequency bandwidth into discrete bands (accordingly named as the resonance and non-resonance frequency bands) and progressively estimates the FRF bounds band by band. After breaking down into discrete bands, two scenarios exist. For the resonance frequency bands, a two-stage application of PCE is required, namely, for the natural frequency and FRF predictions whereas classical PCE can be

applied for frequencies in the latter non-resonance band. Therefore, one requirement of this approach is firstly eligibility by calculation of the natural frequencies and then subsequently FRF of the structure. In this regard, the finite element (FE) method is utilized. It should also be noted that collocation point method is used to evaluate the deterministic coefficients of PCE for the uncertain response. The steps of the approach are illustrated for a single mode of the structure as a flow diagram in Fig. 2 and details are presented with steps below:

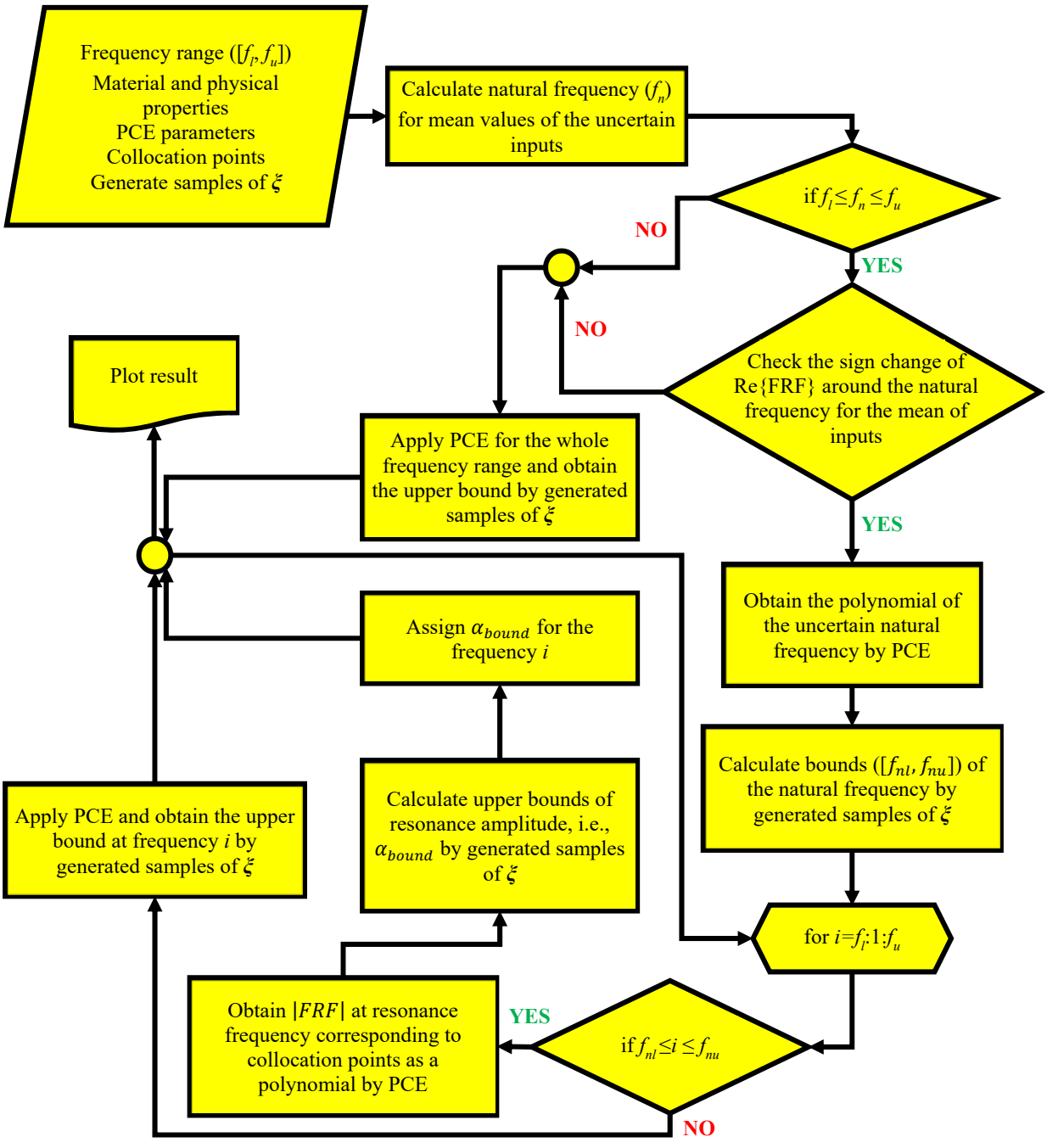

Figure 2. Flow diagram of the presented approach

1. Natural frequencies ($\mathbf{f_n}$) of the structure for the mean values of uncertain inputs are determined to check the existence of a mode in the frequency range considered [f_l, f_u].
2. For no modes in the considered frequency range, PCE technique may be applied for the FRF at each frequency of whole frequency range to obtain the resulting polynomial.
3. To evaluate the bounds of the FRF, the samples of the uncertain parameters (ξ) generated within a 99% confidence interval in accordance with the uncertain parameter distributions, are fed to the resulting polynomial and the samples of the FRFs are evaluated. The upper/lower bounds of the results are calculated by selecting the maximum/minimum of the resulting samples or plotting the probability density function of the response. Even though the bounds are determined by a sampling-based manner, the method is still quicker than MCS.

   Alternatively, one may also determine the bounds within a confidence interval of the resulting distribution for the response by using the statistical moments of the resulting polynomial and the Pearson model without sampling the uncertain parameters. However, for this process, the distribution type should be verified by using higher order standardized statistical moments for each frequency. It may be a tedious task to do this and will decrease the efficiency of the approach. For the further information about the Pearson model, one may refer to Ref. [29].
4. If there is a natural frequency in the frequency range considered [f_l, f_u], the occurrence of the resonance peak at a response point must be checked. Albeit there is a natural frequency within the frequency range [f_l, f_u], the natural frequency may not be observed as a resonance peak in the FRF due to either the excitation or response point coinciding with a nodal point (i.e., the second natural frequency a simply supported beam is not observed as a peak in the FRF if the response is measured at the mid-point of the beam). The real part or imaginary

part of the FRF at the response point may be a good indicator of whether a resonance is likely and hence a resonance peak might occur in the response. Here, the real part of the FRF is utilized, by checking for a sign change of the real part of the FRF around the resonance frequency. Consider the real and amplitude receptances obtained from two different response points with respect to frequency of a structure having a natural frequency at the frequency f_n, presented in Fig. 3.

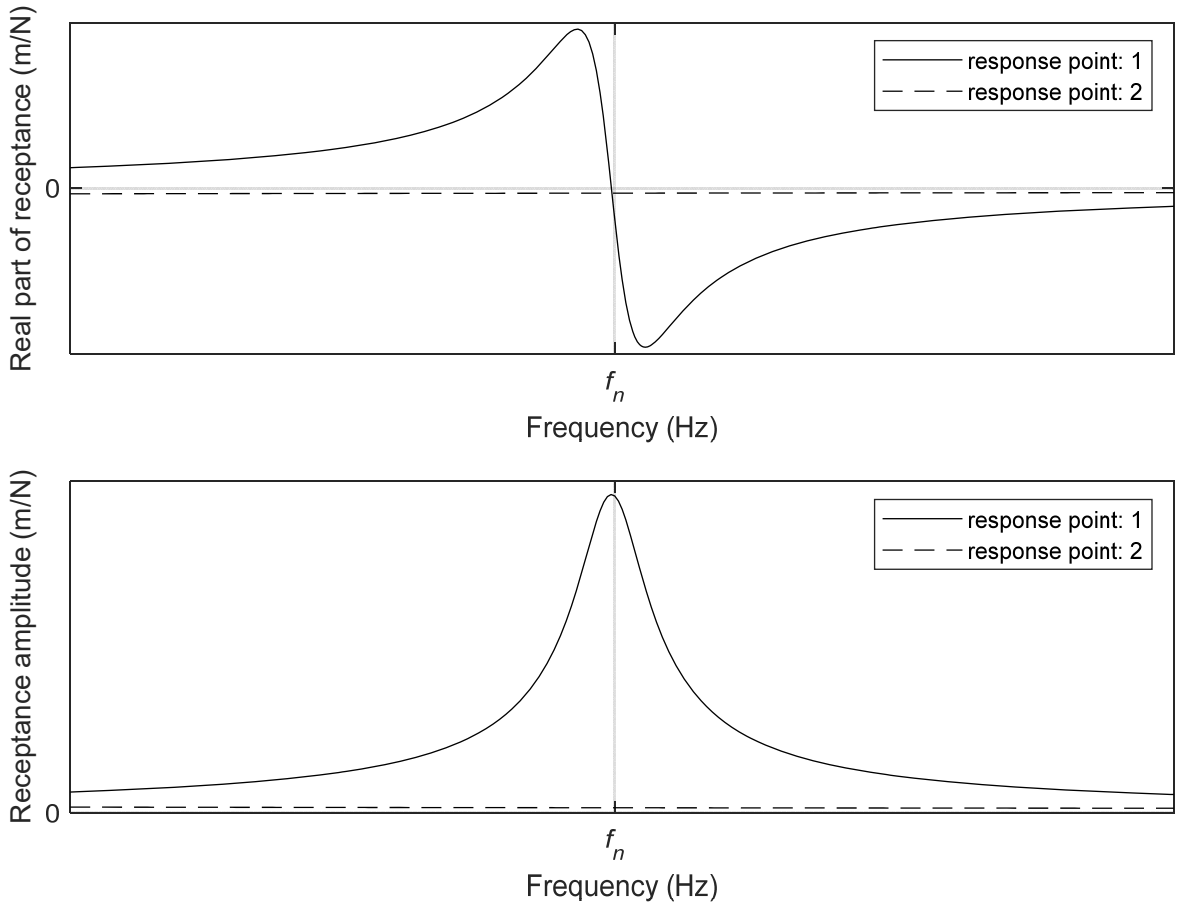

Figure 3. Real part (top) and amplitude (bottom) of displacement with respect to frequency of a structure obtained from two different response points

As may be observed from Fig. 3, if the sign of the real part of the FRF changes in the vicinity of the natural frequency (f_n), it is observed as a peak in FRF-frequency plot. If the sign does not change around the natural frequency, it means the response point is a nodal point.

Therefore, only the natural frequencies with a sign change in the real part of the deterministic FRF must be considered as the excited modes.

5. For the modes which are observed as peaks in the FRF at the response point, the uncertainty in the natural frequency is analysed via PCE by utilizing the collocation points. Then, one may easily determine the lower and upper limits of the natural frequencies, $\left[\mathbf{f}_{nl}, \mathbf{f}_{nu}\right]$ after obtaining the PDF of natural frequencies as presented by a blue line in Fig. 4, by implementing Step 3. These natural frequency bounds yielded are used to identify any resonance bands for the uncertain structure.

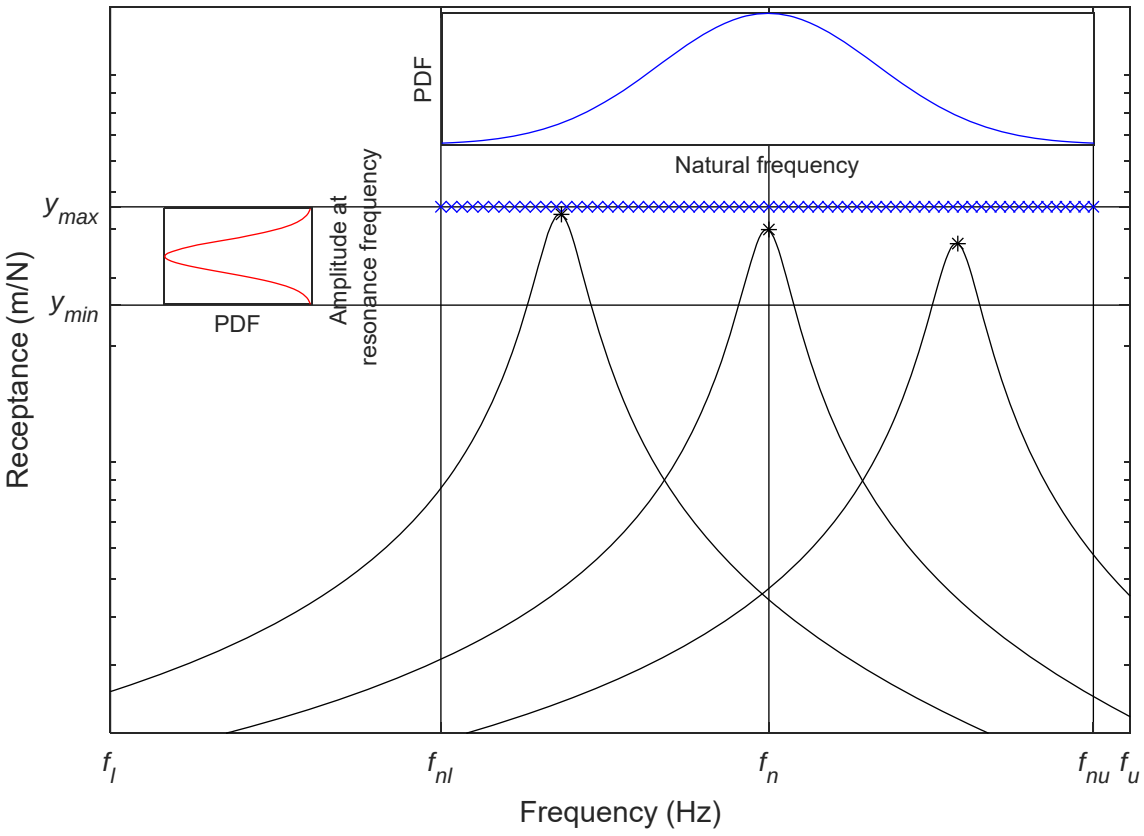

Figure 4. An idealised example of determining the bounds of the amplitude at a resonance band with three collocation points (black: samples used in PCE, black *: resonance amplitude of uncertain samples, blue line: probability density function estimated from natural frequency samples obtained by PCE, red: PDF of the response amplitudes at the resonance frequency obtained by PCE, blue x: estimated resulting bounds)

6. For the frequencies outside of the resonance frequency band (called the non-resonant frequency bands), steps 2-3 may be implemented to evaluate upper bounds whereas steps 7-9 are implemented for the resonant band.
7. The natural frequencies corresponding to the collocation points are calculated.
8. The vibration amplitudes at the uncertain natural frequencies obtained corresponding to the collocation points are determined via FE computations (black asterisks in Fig. 4).
9. Then, the vibration amplitudes obtained in step 8, are utilized as the realizations corresponding to the collocation points in PCE for quantifying uncertain vibration magnitudes at the resonance frequencies and the deterministic coefficients in PCE are calculated for the uncertain vibration amplitude at the resonance frequencies. The PDF (red line in Fig. 4) and upper bound of amplitude (blue 'x' mark in Fig. 4) corresponding to the resonance frequencies are calculated and these are assigned for the frequencies between $\left[\mathbf{f}_{nl}, \mathbf{f}_{nu}\right]$.

So, it is clear from Steps 7-9 that, for a whole resonance band, the amplitude bound is calculated by the two-stage PCE implementation just once. Because the amplitude bound of the resonance band is determined using of the amplitude at the uncertain natural frequency. The term "two-stage PCE implementation" is used, because firstly the natural frequency bound corresponding to the collocation point set is determined in the first stage and then, the natural frequencies corresponding to collocation point set are utilized as inputs for the whole band for amplitude bound determination in the second stage.

3 NUMERICAL STUDIES

In this study, uncertain free and forced vibration analyses of a thin beam are performed via PCE. The numerical model of the structure is constructed via the Finite Element (FE) method.

The boundary condition of the structure is assumed to be fixed-free. Mechanical and physical properties of the considered beam are presented in Table 1.

3.1 Verification study

Before going through the details of the uncertainty analysis, firstly the numerical model of the beam constructed by FE is verified with wave finite element (WFE) numerical simulations and experiments. In this regard, the beam is excited by 1 N flexural point excitation in numerical computations. In the experiments, the schematics shown in Fig. 5 are utilized and excitation is applied at x=0.05 m and the measurements are taken at x=0.4 m between 1-1000 Hz. The length of the elements is assumed to be 0.05 m in the FE and WFE. The calculated results are presented in Fig. 6.

Table 1. Physical and mechanical properties of the beam.

Property (unit)	**Mean value**
Cross-section (m x m)	0.02 x 0.02
Length (m)	0.5
Young modulus (GPa)	62
Density (kg/m^3)	2600
Loss factor	0.005

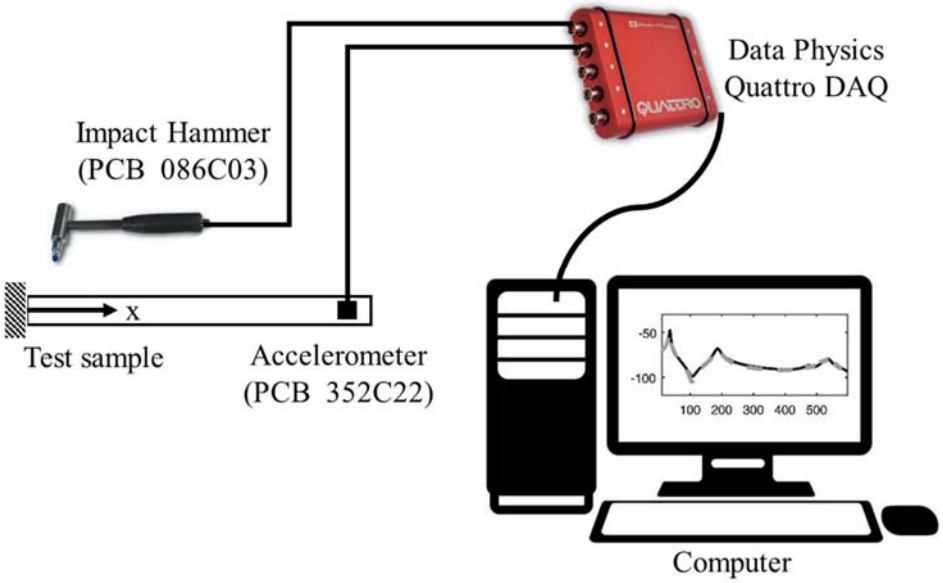

Figure 5. Experimental scheme for impact testing

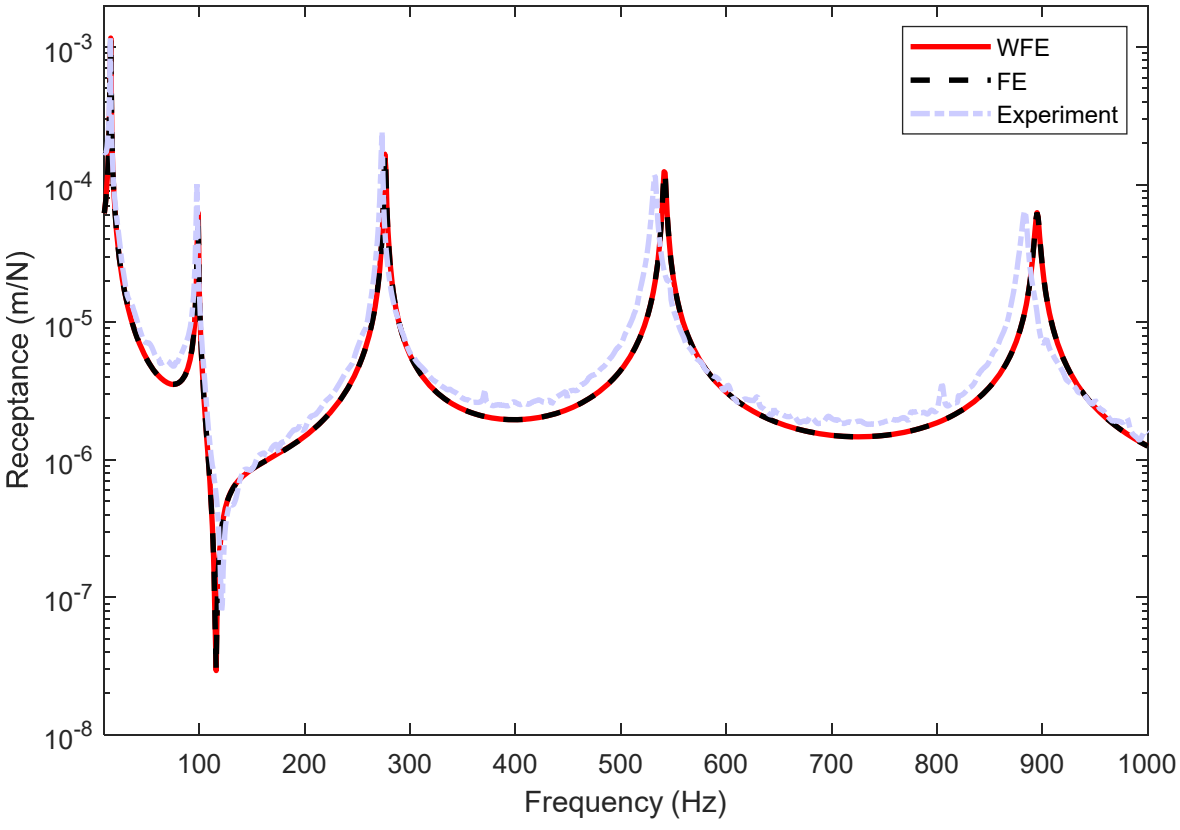

Figure 6. Transfer receptance of the deterministic fixed-free beam

One may infer from Fig. 6 that the FE results are very consistent with both the WFE computations and experimental measurements. However, the measured third to fifth peaks deviate from the numerical simulations, but these are fairly negligible differences due to the difficulty of realising a perfectly rigid or clamped boundary practically. Further calculations or FE model updating may be performed to have a better consistency in the results.

3.2 Uncertainty analysis

In the study, two uncertain cases are considered, i.e., i) a locally uncertain thin beam, and ii) a globally uncertain thin beam.

3.2.1 Locally uncertain beam

In this part of the study, the local uncertainty is created on the cantilever beam by adding variable lumped masses to the tip of the beam. The uncertainty of the lumped mass is assumed to be uniformly distributed between 0-0.020 kg, i.e., $U(0,0.02)$ kg. For the uncertain structure, firstly, the modal analysis was performed via FE-Monte Carlo Simulations with 200 samples for the natural frequency and mode shape samples for the first five modes. These are presented together with the deterministic mode shape and deterministic natural frequency in Fig. 7. The mode shapes have been normalized so that the scalar product of the mode shape vector with itself equals unity to avoid the usage of the deterministic/sample mass matrix.

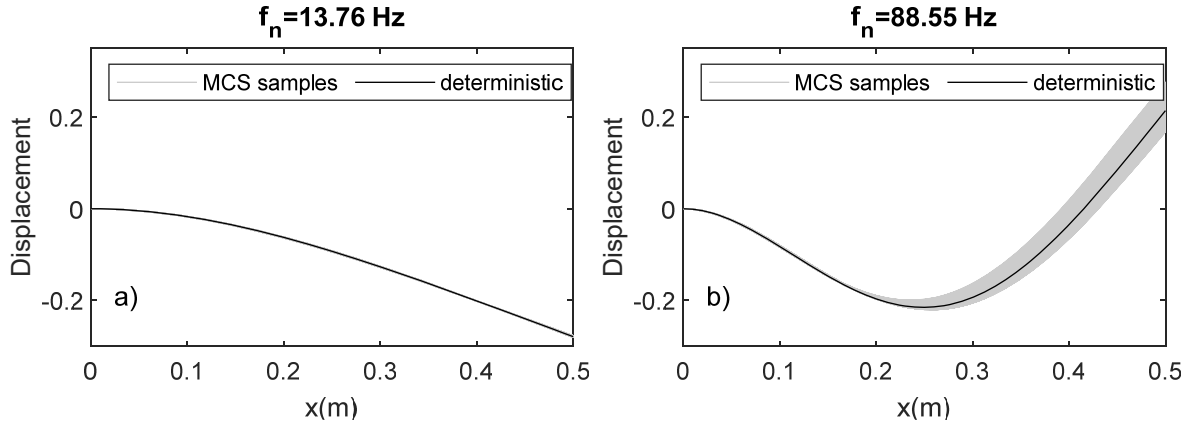

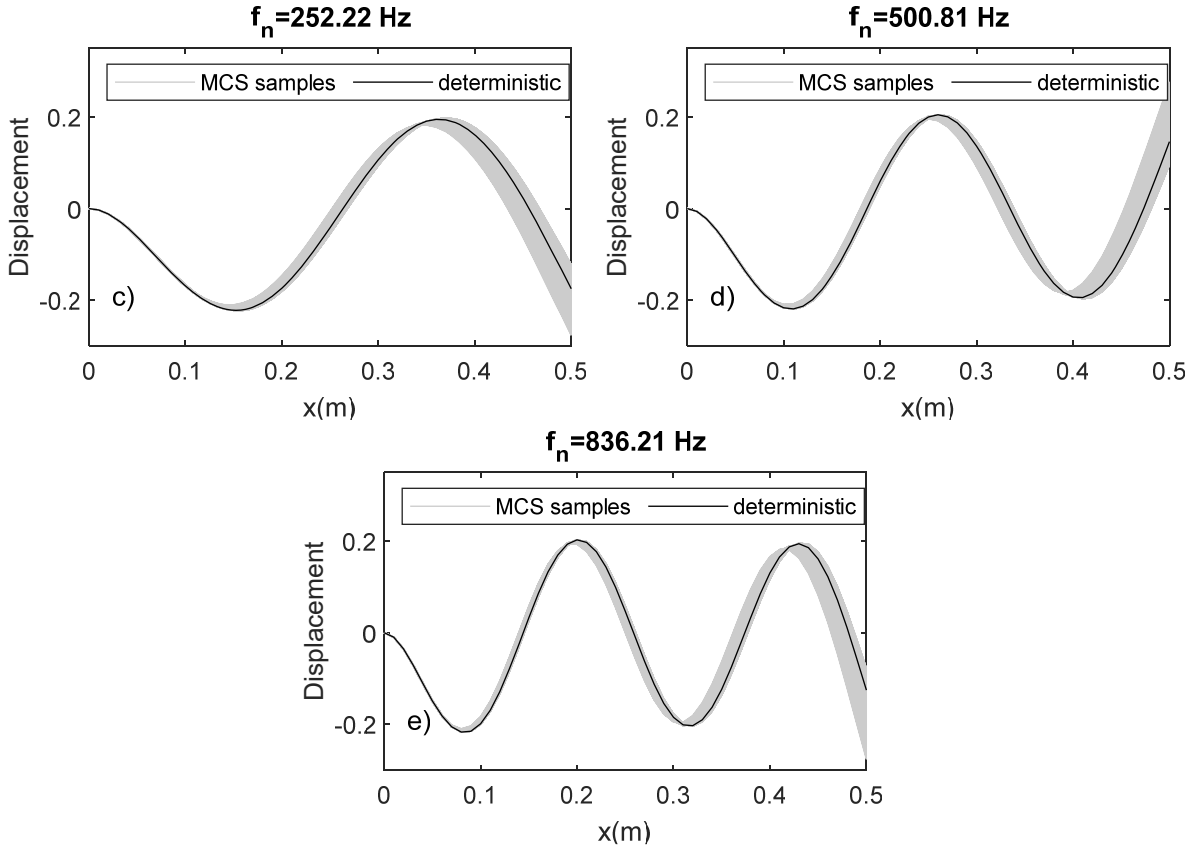

Figure 7. a) The first, b) the second, c) the third, d) the fourth and e) the fifth mode shape of the uncertain beam calculated by FE-MCS

It is observed from Fig. 7 that the change in the mass at the boundary results in increasingly higher uncertainty above the second mode. Besides, the uncertainty increases when the response position gets closer to free end of the structure where the local uncertainty was introduced.

In the natural frequency calculations, the parameters of PCE are selected as n=1 and p=3 in the natural frequency calculations, so N=3. Since the uncertain mass has the uniform distribution, the uncertain input parameter, ξ is also uniformly distributed between -1 and 1. The uncertain mass at the boundary, natural frequencies and FRF are described by using Legendre polynomials. The vector that contains the polynomial terms is $P=\left\{1 \quad \xi \quad 1.5\xi^2-0.5 \quad 2.5\xi^3-1.5\xi\right\}$. The number of collocation point is selected as N+1 for whole calculations where they are selected by the roots of the fourth order Legendre polynomial

as $\xi = \{-0.34, -0.8611, 0.34, 0.8611\}$. The deterministic polynomial coefficients of the first five natural frequencies are presented in Table 2.

Table 2. Deterministic polynomial coefficients obtained for the first five natural frequencies

Mode Number	x_0	x_1	x_2	x_3
1	13.86	-1.67	0.20	-0.02
2	89.36	-7.23	1.67	-0.33
3	254.52	-15.24	4.82	-1.26
4	505.01	-23.21	8.97	-2.81
5	842.57	-30.82	13.67	-4.83

As observed from Table 2, the absolute value of the deterministic coefficients converges to zero as the order of the terms increases. The normalized histograms of the resulting natural frequencies for the first five modes are obtained by sampling the uncertain input parameter using 200 samples for the assumed uniformly distributed point mass. The results are compared with MCS for two different numbers of samples, i.e., 200 and 10000 samples. This was performed and utilized to show the sampling size is sufficient in the uncertainty modelling. The results are compared with MCS in Fig. 8. Note that, the normalization of histograms is performed so that the area under the curve or sum of rectangular areas are equal to 1.

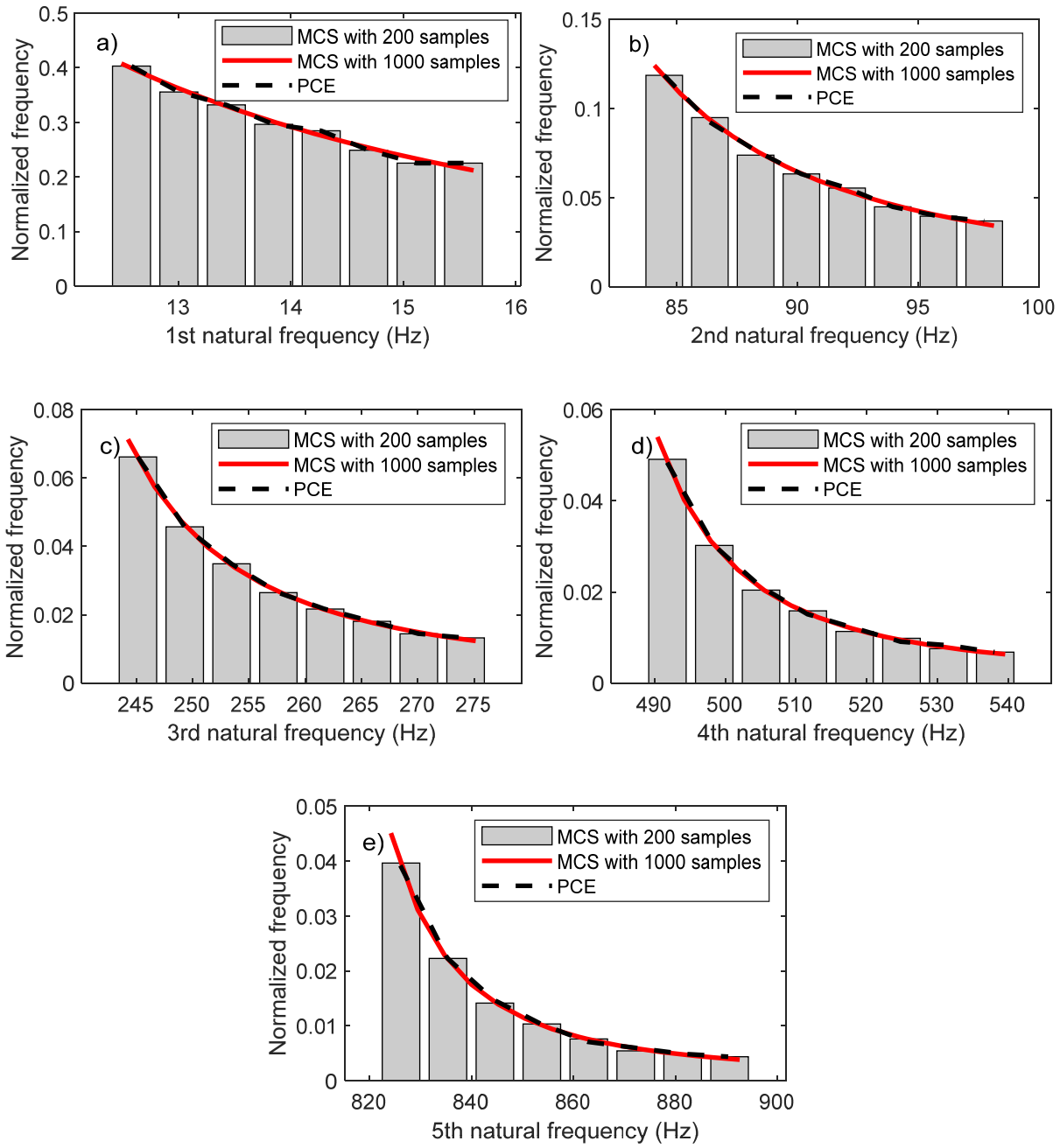

Figure 8. Comparison of the normalized histograms for the five lowest order natural frequencies

As seen from Fig. 8, the PCE and MCS results are consistent and in good agreement with each other. On the other hand, MCS with 200 samples converged to MCS results using 10000 samples; therefore one may conclude that 200 samples are enough for the modelling of the uniform distribution. Moreover, the form of the normalized histograms belonging to the first

natural frequency is nearly linear, and the behaviour of the curves are changing slightly with the increasing mode order. The histogram of the natural frequency appears to follow the form of the reciprocal of the square root function due to the local addition of the uncertain tip mass. From Fig. 8, one may also observe the bounds of the natural frequencies and resonance bands, which is determined from the frequencies within these bounds. For these bands, the steps 7-9 in the introduced approach mentioned in Section 2.4 will be applied.

Next, the effect of structural uncertainty on the forced response spectra is examined. The bounds of the uncertain FRF are calculated by the introduced approach with PCE parameters n=1 and p=3. The results are compared with the experiments and numerical FE-MCS by 200 uncertain samples of the additional lumped mass. In the experiments, the masses are attached to the free end of the cantilever beam in accordance with a uniform distribution between 0-0.020 kg by generating 20 samples by using adhesive sticky putty. It should be noted that this will also introduce damping uncertainty seen in the subsequent measured response spectra. Due to adding adhesive putty, the loss factor of the beam is assumed to be 0.015 in the simulations. The experiments were performed twice to check the repeatability. Apart from the introduced approach, the mean and the upper bounds of the response are also calculated by PCE computations with n=1, p={3, 10}. The uncertain transfer receptance at x=0.4 m corresponding to the excitation at x=0.05 m is presented in Fig. 9. Note that, the upper bounds of the FE-MCS are presented rather than the individual prediction response samples for clarity of the results shown in Fig. 9. The relative discrepancy of the bounds calculated by proposed approach and classical PCE compared to FE-MCS are calculated by $\left|W_{PCE}^{bound} - W_{MCS}^{bound}\right|$ and presented in Fig. 10.

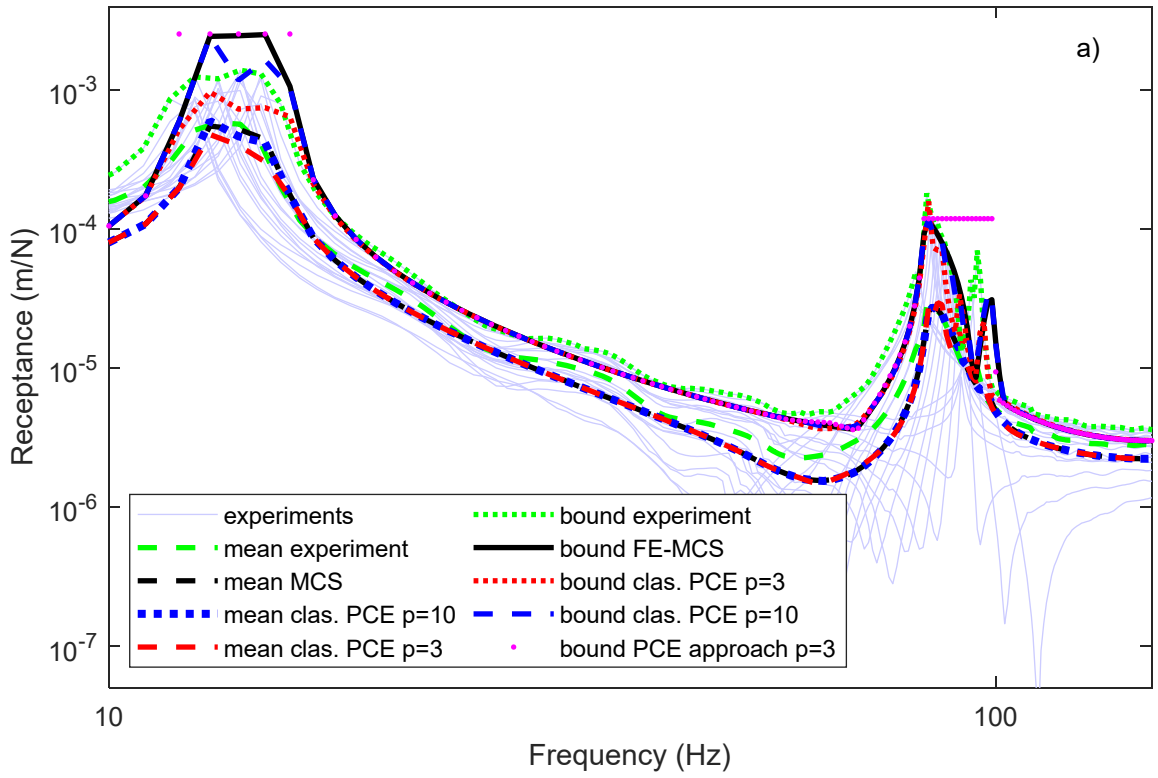
a)
Receptance (m/N)
Frequency (Hz)
experiments
mean experiment
mean MCS
mean clas. PCE p=10
mean clas. PCE p=3
bound experiment
bound FE-MCS
bound clas. PCE p=3
bound clas. PCE p=10
bound PCE approach p=3

1

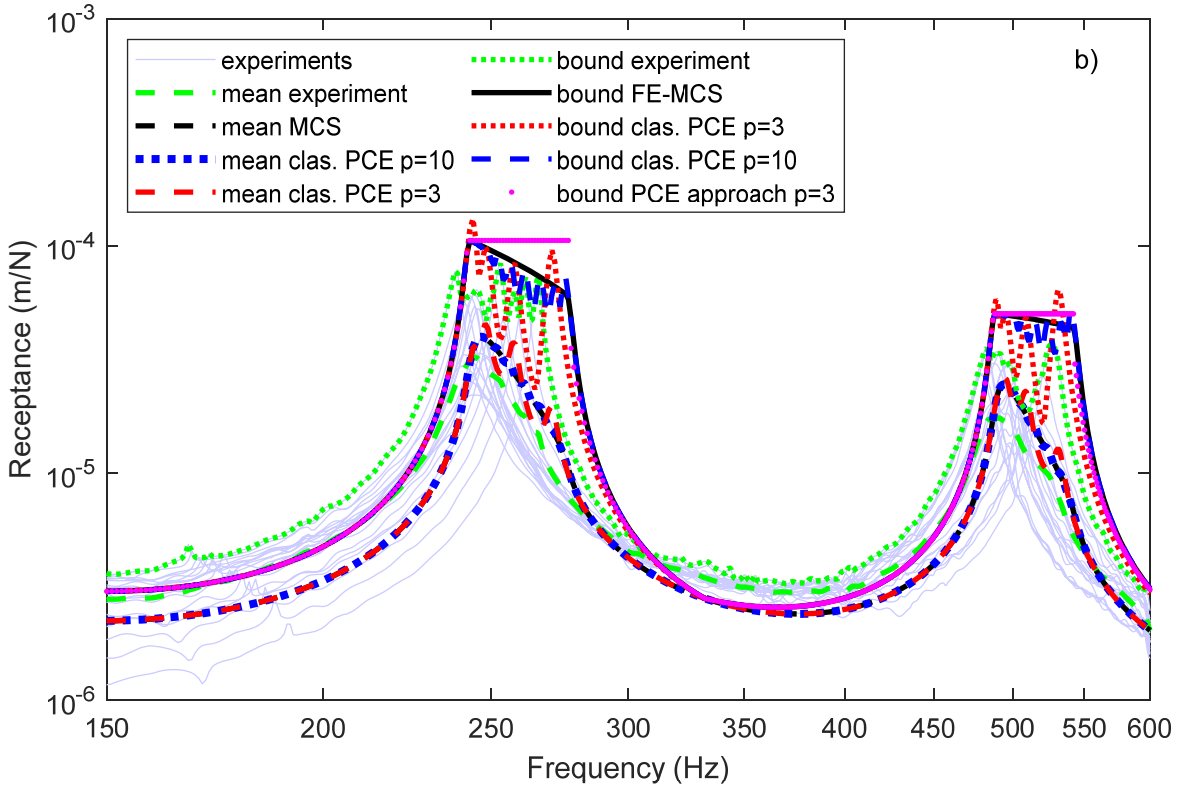
b)
Receptance (m/N)
Frequency (Hz)
experiments
mean experiment
mean MCS
mean clas. PCE p=10
mean clas. PCE p=3
bound experiment
bound FE-MCS
bound clas. PCE p=3
bound clas. PCE p=10
bound PCE approach p=3

2

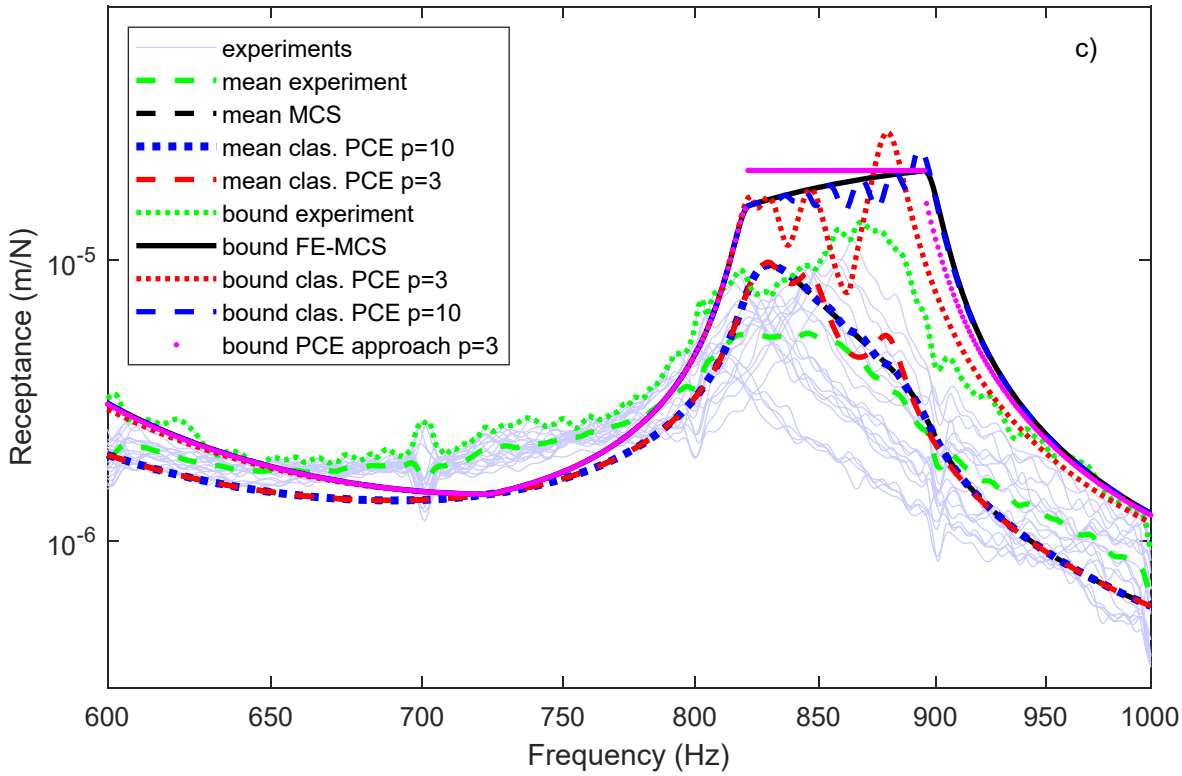

Figure 9. Transfer receptance at x=0.4 m, excitation at x=0.05 m, for the cantilever beam possessing local mass uncertainty at the free end, between a) 10-150 Hz, b) 150-600 Hz and b) 600-1000 Hz

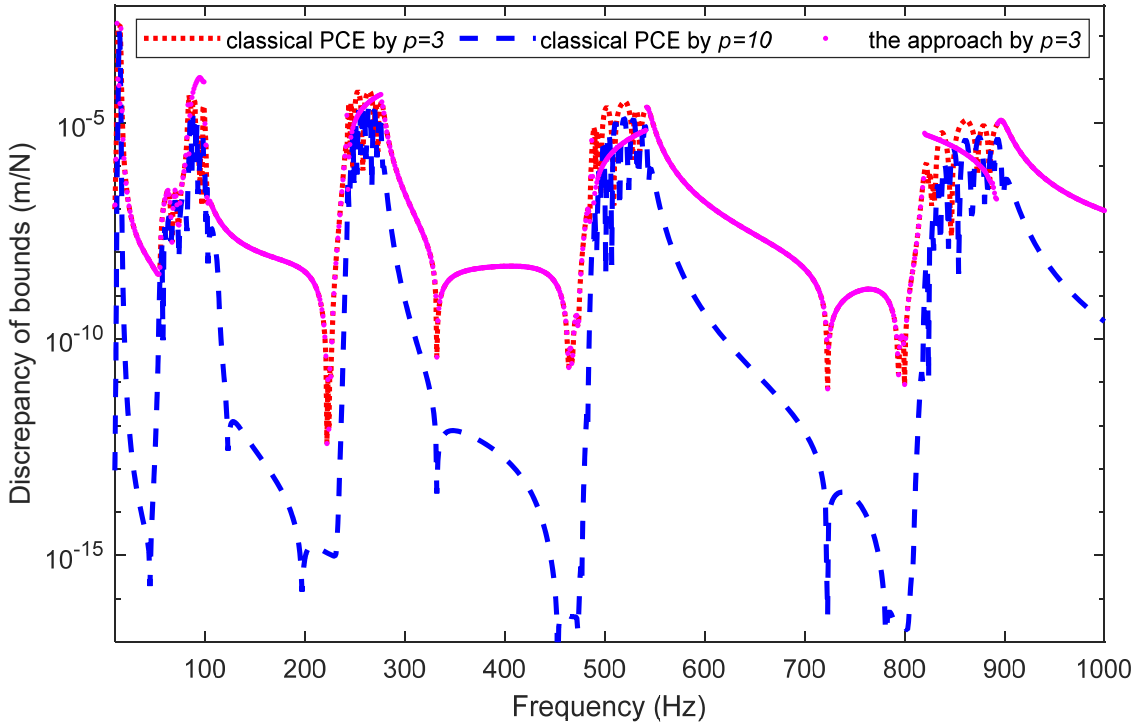

Figure 10. Discrepancy of the classical PCE and the present approach compared to the FE-MCS in terms of receptance bounds

Fig. 9 shows that the experimental results are mostly consistent with numerical simulations. The discrepancies in the experimental results, presented in Fig. 9, may be due to the number of samples and/or additional damping of the adhesive putty. However, the mean FRF calculated by FE-PCE with p=3 shows oscillations about the mean of FE-MCS in the resonance bands of higher order modes, but these oscillations are not observed for FE-PCE with p=10 and it converges to the FE-MCS and physical experiments. On the other hand, when the upper bounds of the FRF is of interest, FE-MCS is clearly able to estimate the bounds of the response, as expected. If the bounds of the FE-MCS is taken as a reference, FE-PCE with both p=3 and p=10 exhibit higher amplitude variations compared to the variations around the mean. These are most likely because of the variation in the higher order central statistical moments (variance etc.) of the response. Besides, the approach presented in the study is clearly able to estimate the upper bounds with lower order PCE, i.e., p=3. As the discrepancy of the PCE results presented in Fig. 10 is of interest, it is clearly seen that the proposed approach has lower error than the classical PCE with p=3 at most frequencies. The simulation time for the FE-MCS, the proposed PCE approach with p=3, and the FE-PCE with p=3 and with p=10 are 39 s, 5.5 s, 4 s and 10 s, respectively. These results indicate that FE-PCE with the higher order for the mean response and the introduced approach with lower order polynomial for the bound calculation may be suitable and acceptable alternative methods for dynamic predictions of structures possessing local uncertainties.

3.2.2 Globally uncertain beam

The approach is now assessed for the beam possessing global uncertainty. In this regard, the Young's modulus of the cantilever beam is assumed to be uncertain with a normal distribution in GPa given by $N(70,3.5)$. The uncertain parameter (ξ) is assumed to have unit normal

distribution i.e. $N(0,1)$. The FRF is described using Hermite polynomials, whereas the Young's modulus is expressed in terms of the uncertain input variable as given in Eq. (9). The samples of the uncertain parameter (ξ) required to calculate the bounds are generated within the limits of [-3,3] which corresponds to the 99% confidence interval. The uncertain FRF upper bounds are calculated with the proposed approach described in Section 2.4 with the PCE parameters of n=1 and p=4. Since N=4, the collocation points are selected by the roots of the fifth order Hermite polynomial as $\xi = \{-2.857, -1.3556, 0, 1.3556, 2.857\}$. The bounds and mean of FRF are determined via the FE-PCE with p=10, whereas only the mean FRF is calculated via FE-PCE with p=10 and the 5th order (r=5) Shank's transformation. The uncertain transfer receptance at x=0.4 m corresponding to the excitation at x=0.05 m is compared by FE-MCS using 10000 samples in Fig. 11. Since there is no adhesive putty addition in this case, the loss factor is again assumed to be as 0.005 as in the simulations.

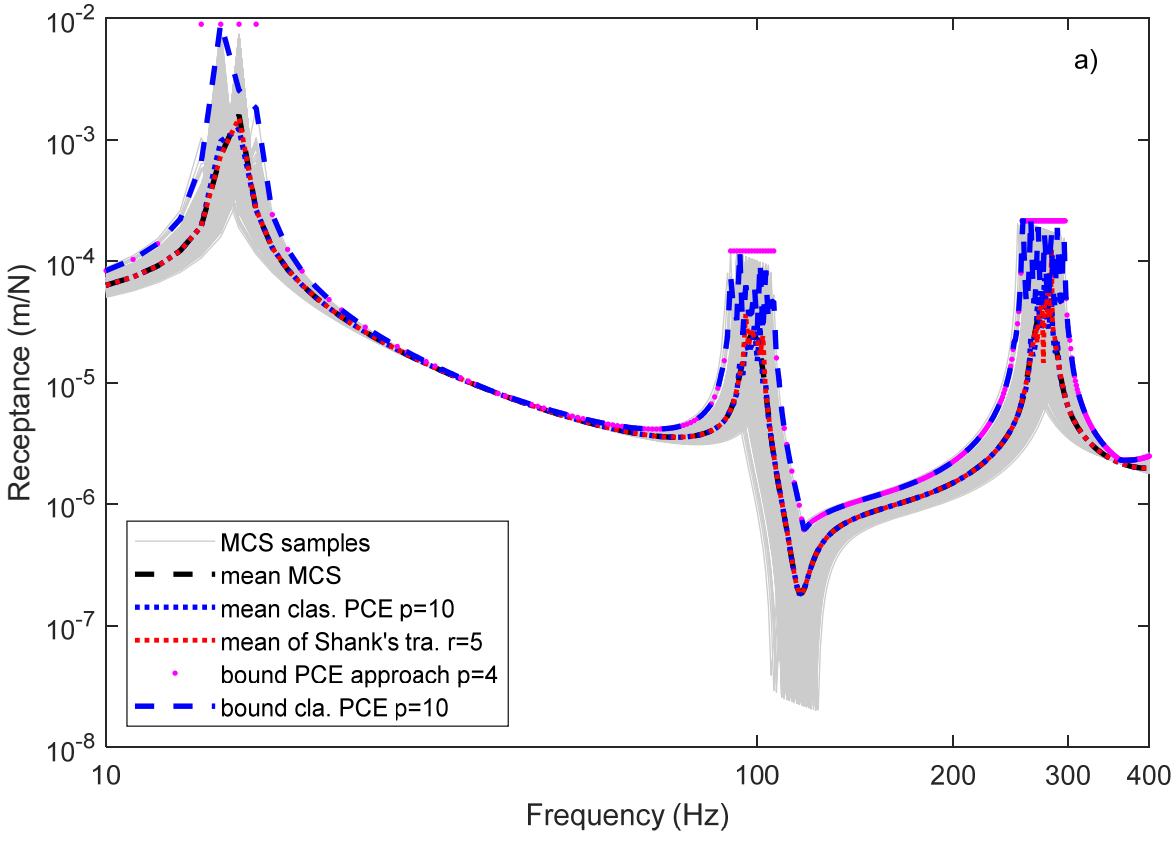

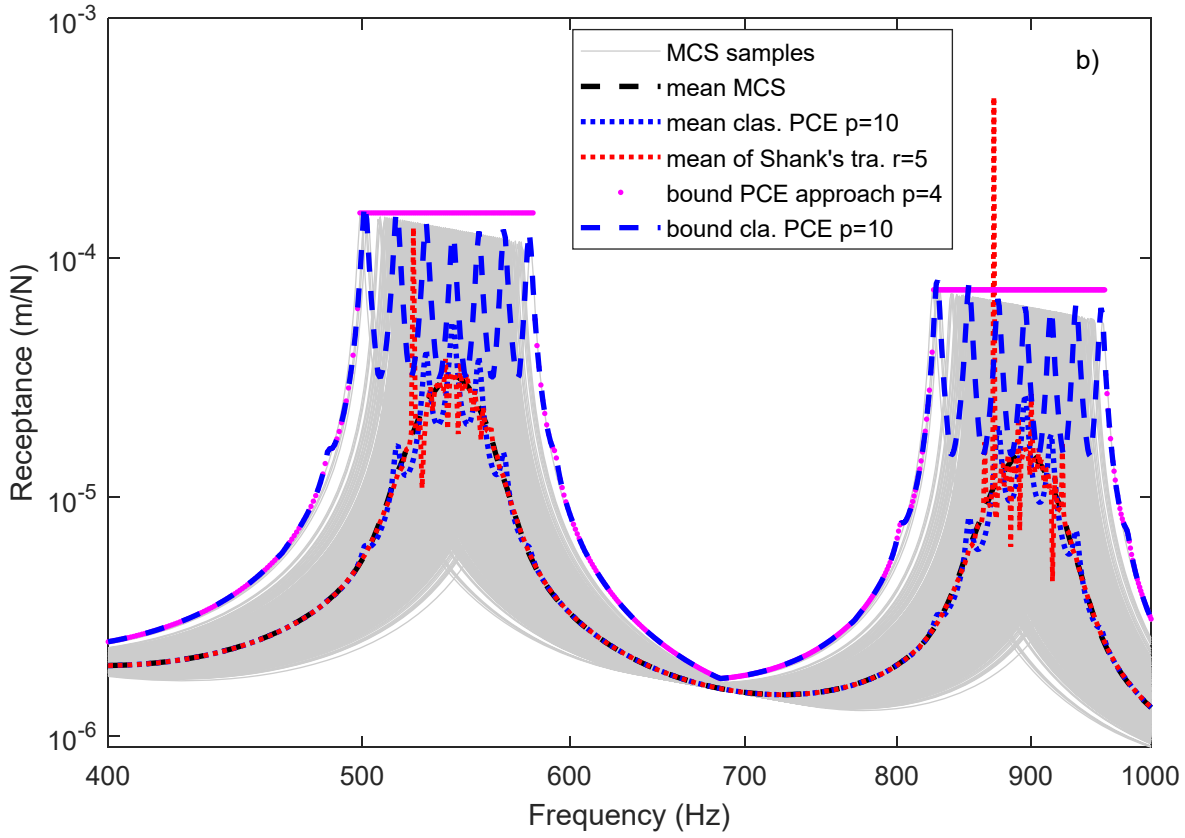

Figure 11. Transfer receptance at x=0.4 m, excitation at x=0.05 m, for the cantilever beam possessing global uncertainty between a) 10-400 Hz and b) 400-1000 Hz

The following conclusions may be inferred from Fig. 11:

1. The higher order PCE has oscillations around the desired response in the resonance bands (mean FRF or FRF bounds) as depicted in the lower order PCE of local uncertainty problem in Fig. 9. Therefore, it may be concluded that, the optimum number of the polynomial order may change for the same structure corresponding to the different input uncertain parameter. One other cause that affects the convergence of PCE is having lower damping of the globally uncertain problem than the local uncertain problem.
2. PCE with Shank's transformation increases the rate of the convergence to the mean value. However, it also results in some problematic responses at certain frequencies in the resonance bands. The inaccuracy may be due to not having a slight change between the rows

of nominator or denominator in Eq. (13), which will yield a zero determinant for any of them. Increasing the order of the polynomial and the transformation may be a solution to this problem as reported by Jacquelin et al. [11].

3. The relative solution time for the problem is 13 s for PCE with p=10 without the transformation, 7 s for the proposed PCE bound approach, approximately 2000 s for MCS with 200 samples and 134 s for Shank's transformation.
4. PCE approach with/without the transformation could not estimate the uncertain response successfully. On the other hand, the approach introduced with the utilized polynomial orders is really successful. This makes the approach efficient compared to MCS and PCE with/without transformation in terms of computational load. Hence, it may be used for more complex problems.

4 CONCLUSION

In the literature there exists different transformations for the purpose of accelerating the convergence in PCE aiming for the statistical moments of the response around resonance for lightly damped and uncertain structures. However, these transformations work well if the order of the polynomials and transformation are quite high. In this paper, an upper bound estimation of the uncertain frequency response function (FRF) is performed with low order Polynomial Chaos Expansion (PCE) without any transformation. In this regard, the approach breaks the whole frequency range into bands, namely the resonance and non-resonance bands, by calculating the natural frequency bounds of the uncertain structure and progressively calculating the upper FRF bounds for those bands. For the non-resonance band, the FRF bounds are calculated by classical PCE implementation at each frequency, whereas PCE is implemented for FRF amplitudes at the uncertain natural frequencies. The approach is tested for two cases i.e., the beams possessing local and global uncertainty, respectively. The results

are compared with experiments, Monte Carlo simulation and PCE with/without transformation. It is observed that the approach is successful with the application of a lower order PCE, even though the cases where PCE with/without transformation fails.

ACKNOWLEDGEMENTS

This study is supported by "The Scientific and Technological Research Council of Turkey, TUBITAK" through the 2219-International Postdoctoral Research Fellowship Program for Turkish citizens.

REFERENCES

[1] R.Y. Rubinstein, D.P. Kroese, Simulation and the Monte Carlo Method, 3th ed., John Wiley & Sons, New Jersey, 2016.

[2] R.E. Moore, Methods and applications of interval analysis, Society for Industrial and Applied Mathematics, Philadelphia, 1979.

[3] R. Santoro, G. Failla, G. Muscolino, Interval static analysis of multi-cracked beams with uncertain size and position of cracks, Appl Math Model. 86 (2020) 92–114. https://doi.org/10.1016/j.apm.2020.03.049.

[4] I. Elishakoff, R.T. Haftka, J. Fang, Structural design under bounded uncertainty—Optimization with anti-optimization, Comput Struct. 53 (1994) 1401–1405. https://doi.org/10.1016/0045-7949(94)90405-7.

[5] C.K. Choi, H.H. Yoo, Uncertainty analysis of nonlinear systems employing the first-order reliability method, Journal of Mechanical Science and Technology. 26 (2012) 39–44. https://doi.org/10.1007/s12206-011-1011-x.

[6] S.H. Lee, B.M. Kwak, Response surface augmented moment method for efficient reliability analysis, Structural Safety. 28 (2006) 261–272. https://doi.org/10.1016/j.strusafe.2005.08.003.

[7] R.G. Ghanem, P.D. Spanos, Stochastic finite elements: A spectral approach, Dover Publications, New York, 2003.

[8] A. Manan, J.E. Cooper, Prediction of uncertain frequency response function bounds using polynomial chaos expansion, J Sound Vib. 329 (2010) 3348–3358. https://doi.org/10.1016/J.JSV.2010.01.008.

[9] S.K. Choi, R. v. Grandhi, R.A. Canfield, C.L. Pettit, Polynomial chaos expansion with latin hypercube sampling for estimating response variability, AIAA Journal. 42 (2004) 1191–1198. https://doi.org/10.2514/1.2220.

[10] J. Henneberg, J.S. Gomez Nieto, K. Sepahvand, A. Gerlach, H. Cebulla, S. Marburg, Periodically arranged acoustic metamaterial in industrial applications: The need for uncertainty quantification, Applied Acoustics. 157 (2020) 107026. https://doi.org/10.1016/j.apacoust.2019.107026.

[11] E. Jacquelin, S. Adhikari, J.J. Sinou, M.I. Friswell, Polynomial chaos expansion in structural dynamics: Accelerating the convergence of the first two statistical moment sequences, J Sound Vib. 356 (2015) 144–154. https://doi.org/10.1016/j.jsv.2015.06.039.

[12] E. Jacquelin, S. Adhikari, J.-J. Sinou, M.I. Friswell, Polynomial Chaos Expansion and Steady-State Response of a Class of Random Dynamical Systems, J Eng Mech. 141 (2015) 04014145. https://doi.org/10.1061/(asce)em.1943-7889.0000856.

[13] K. Sepahvand, S. Marburg, H.-J. Hardtke, Uncertainty quantification in stochastic systems using polynomial chaos expansion, Int J Appl Mech. 02 (2010) 305–353. https://doi.org/10.1142/S1758825110000524.

[14] K. Sepahvand, Spectral stochastic finite element vibration analysis of fiber-reinforced composites with random fiber orientation, Compos Struct. 145 (2016) 119–128. https://doi.org/10.1016/j.compstruct.2016.02.069.

[15] K. Dammak, S. Koubaa, A. el Hami, L. Walha, M. Haddar, Numerical modelling of vibro-acoustic problem in presence of uncertainty: Application to a vehicle cabin, Applied Acoustics. 144 (2019) 113–123. https://doi.org/10.1016/J.APACOUST.2017.06.001.

[16] A. Sarkar, R. Ghanem, A substructure approach for the midfrequency vibration of stochastic systems, J Acoust Soc Am. 113 (2003) 1922. https://doi.org/10.1121/1.1558374.

[17] A. Sarkar, R. Ghanem, Mid-frequency structural dynamics with parameter uncertainty, Comput Methods Appl Mech Eng. 191 (2002) 5499–5513. https://doi.org/10.1016/S0045-7825(02)00465-6.

[18] D. Sarsri, L. Azrar, A. Jebbouri, A. el Hami, Component mode synthesis and polynomial chaos expansions for stochastic frequency functions of large linear FE models, Comput Struct. 89 (2011) 346–356. https://doi.org/10.1016/j.compstruc.2010.11.009.

[19] K. Sepahvand, S. Marburg, H.-J. Hardtke, Numerical solution of one-dimensional wave equation with stochastic parameters using generalized polynomial chaos expansion, Journal of Computational Acoustics. 15 (2007) 579–593. https://doi.org/10.1142/S0218396X07003524.

[20] A. Seçgin, M. Kara, N.S. Ferguson, Discrete singular convolution–polynomial chaos expansion method for free vibration analysis of non-uniform uncertain beams, JVC/Journal of Vibration and Control. 28 (2022) 1165–1175. https://doi.org/10.1177/1077546320988190.

[21] K. Sepahvand, S. Marburg, Identification of composite uncertain material parameters from experimental modal data, Probabilistic Engineering Mechanics. 37 (2014) 148–153. https://doi.org/10.1016/J.PROBENGMECH.2014.06.008.

[22] K. Sepahvand, Stochastic finite element method for random harmonic analysis of composite plates with uncertain modal damping parameters, J Sound Vib. 400 (2017) 1–12. https://doi.org/10.1016/j.jsv.2017.04.025.

[23] K. Sepahvand, M. Scheffler, S. Marburg, Uncertainty quantification in natural frequencies and radiated acoustic power of composite plates: Analytical and experimental investigation, Applied Acoustics. 87 (2015) 23–29. https://doi.org/10.1016/j.apacoust.2014.06.008.

[24] G. Blatman, B. Sudret, Adaptive sparse polynomial chaos expansion based on least angle regression, J Comput Phys. 230 (2011) 2345–2367. https://doi.org/10.1016/J.JCP.2010.12.021.

[25] V. Keshavarzzadeh, R.G. Ghanem, S.F. Masri, O.J. Aldraihem, Convergence acceleration of polynomial chaos solutions via sequence transformation, Comput Methods Appl Mech Eng. 271 (2014) 167–184. https://doi.org/10.1016/j.cma.2013.12.003.

[26] J.J. Sinou, E. Jacquelin, Influence of Polynomial Chaos expansion order on an uncertain asymmetric rotor system response, Mech Syst Signal Process. 50–51 (2015) 718–731. https://doi.org/10.1016/j.ymssp.2014.05.046.

[27] V. Yaghoubi, S. Marelli, B. Sudret, T. Abrahamsson, Sparse polynomial chaos expansions of frequency response functions using stochastic frequency transformation, Probabilistic Engineering Mechanics. 48 (2017) 39–58. https://doi.org/10.1016/j.probengmech.2017.04.003.

[28] D. Xiu, G.E. Karniadakis, Modeling uncertainty in flow simulations via generalized polynomial chaos, J Comput Phys. 187 (2003). https://doi.org/10.1016/S0021-9991(03)00092-5.

[29] E.S. Pearson, Some Problems Arising in Approximating to Probability Distributions, Using Moments, Biometrika. 50 (1963) 95. https://doi.org/10.2307/2333751.